An Analysis of Tail End Precipitation Events over Time

VU EDS - Rainfall case

B. Spanjers

PCS-29

Sara D'haene (2902715), Sophie Gatsonides (2740284), Lucas Sanders (2902232), Wouter Zaadstra (2823591)

Table of contents

Abstract

This paper contains research on the trend in precipitation, threshold exceedance and joint exceedances of several weather stations throughout Spain. This builds further on the research done by Spanjers et al. (2025) about precipitation and the NAO-index. We therefore use daily data of precipitation of these weather stations together with the daily NAO-index and several papers containing information on this particular subject. The main model we use for this paper is the General Additive Model which is able to model the trend and seasonality of our datasets.

Our main findings contain observations on different trends in the data due to the multiple climates in Spain. Secondly the joint exceedances of spatially correlated weather events did not increase over time following from our GAMs. And lastly we validated each specificated GAM to fit the best one onto our research.

1. Introduction

In September 2019, eastern Spain experienced one of the most destructive flood events in its recent history following an intense DANA (Depresión Aislada en Niveles Altos) episode. Extreme and spatially clustered precipitation caused widespread flooding across the Valencia and Murcia regions. The Spanish Insurance Compensation Consortium reported insured flood losses exceeding EUR 450 million (CCS, 2020), while total economic damages were estimated to surpass EUR 2.2 billion (AON, 2019).

Post-event analyses of the September 2019 DANA confirm that flood losses were driven by the simultaneous occurrence of extreme precipitation across large areas rather than by isolated local rainfall extremes (Author et al., 2022). Such large-scale flood events dominate tail losses and place increasing stress on disaster-risk financing systems, highlighting the importance of spatial dependence in precipitation-related risk (Jongman et al., 2014). These patterns have direct implications for risk management. Joint precipitation extremes cause losses to accumulate across locations, making joint exceedance risk central to insurance and risk transfer. Accurate estimation of exceedance probabilities is therefore essential for index-based and parametric insurance instruments designed to cover spatially correlated climate risk (Vedenov & Barnett, 2004).

For Spain, the potential of spatial diversification has been examined empirically. Martínez-Salgueiro and Tarrazon-Rodon (2021) show that spatial aggregation can substantially reduce systemic precipitation risk, with buffer loads - measured by expected shortfall - declining by up to 67%. However, diversification benefits depend critically on spatial dependence and climatic heterogeneity across regions, in line with documented strong seasonality and mixed evidence on long-term changes in extreme precipitation across Spain (Vicente-Serrano et al., 2011; Senent-Aparicio et al., 2023). This highlights the need to model not only marginal exceedance probabilities, but also the joint occurrence of extremes across stations.

In addition to long-term changes, precipitation extremes are influenced by large-scale atmospheric circulation patterns. In particular, the North Atlantic Oscillation has been shown to modulate the seasonal timing of precipitation over the Iberian Peninsula and is therefore included as a conditioning covariate in extended model specifications (Trigo et al., 2004; Spanjers et al., 2025).

Against this background, this paper addresses the following research questions:

1. *What is the probability that precipitation crosses the 95th wet day percentile at any given day in the year for Spanish weather stations, and is there evidence of this probability changing over time?*
2. *Is there evidence of the daily probability of spatially correlated joint precipitation exceedances above the 95th percentile across Spain changing over time?*

3. *Which weather station pairs exhibit weakest/strongest diversification, and how does this relate to climate regimes?*

2. Data

2.1 Data & Variables

The precipitation data used in this study are obtained from the European Climate Assessment & Dataset (ECA&D). Specifically, we use the non-blended ECA daily precipitation amount for the period 1970–2020 for the stations Alicante, Asturias, Barcelona, Madrid, Sevilla, Valencia and Vigo. A subset chosen to capture Spain's substantial climate heterogeneity, ranging from Oceanic and Mediterranean to Semi-Arid regimes. This panel data consisting of multiple time series includes the following variables: a station identifier (STAID), a daily date column (DATE), daily precipitation (RR), and a quality indicator (Q_RR). Precipitation is recorded in units of 0.1 mm; in the research this will be rescaled to millimetres. Following the ECA&D quality flags, we retain only observations with Q_RR = 0 ("valid") and exclude suspect (1) and missing (9) entries to ensure consistency of the time series used for estimation. Observations marked with the value -9999 were treated as missing and removed from the dataset, a filtering process that excluded an average of 903 out of 18,628 days per station over the 51-year period.

When plotting this data against a normal distribution we can easily conclude non-normality. As shown in **appendix x** the data is horizontal on the left (rainfall is never negative) and very right-skewed with extreme kurtosis in its extremes. A normal distribution consists of a skewness of 0 and kurtosis of 3. Our data has a skewness of 4.63 and kurtosis of 38.63.

Another used variable is the NAO-index is obtained from the Climate Prediction Center, and is available at daily frequency from 1950 onward. The following columns are included: "YEAR", "MONTH", and "DAY", and the NAO index in "AAO_INDEX_CDAS". (covariate)

2.2 Threshold definition

This research defines a wet day as a day with a precipitation amount that is greater than 1 mm, $RR > 0.01$. The binary variable of a wet day is then set to 1, and 0 for $RR < 0.01$. For each weather station, daily precipitation thresholds are defined using station-specific 95th percentile thresholds of daily rainfall, computed conditional on wet days, such that exceedances capture unusually high precipitation, as opposed to the mere occurrence of rainfall. These station-specific thresholds ensure comparability across heterogeneous climates. Based on these thresholds, the daily data is transformed into a binary series, $Y_{s,t}$:

- $Y_{s,t} = 1$, When the daily precipitation exceeds the station-specific threshold, representing an extreme event.
- $Y_{s,t} = 0$, When the precipitation is below the threshold or the day is classified as dry.

2.3 descriptive statistics

In Table 1 the summaries of station-level precipitation characteristics over 1970-2020, including mean daily precipitation, wet-day frequency, station-specific wet-day 95th percentile thresholds, and exceedance rates can be found.

station	mean_rr	wet_share	p95	exc_rate	exc_rate_wet	n_obs	n_years
Alicante	0,831066	0,096328	27,6	0,004805	0,049881	17482	51
Asturias	3,174857	0,361766	26,605	0,018088	0,05	17691	51
Barcelona	1,844717	0,165378	37,63	0,008303	0,050208	17463	51
Madrid	1,09163	0,154515	20	0,007681	0,049708	17707	51
Sevilla	1,498165	0,140851	33,215	0,007048	0,05004	17877	51
Valencia	1,29179	0,121304	38,02	0,006097	0,050258	17551	51
Vigo	5,0433	0,349705	44,185	0,017529	0,050126	18141	51

Table 1

From the table, Atlantic stations exhibit higher rainfall frequency and intensity than Mediterranean and inland stations, while substantial variation in p95 thresholds, such as relatively low mean precipitation but high thresholds in Valencia highlights cross-climatic heterogeneity in extreme rainfall levels.

When looking at the plots of the data in **appendix x** we observe a negative trend in precipitation over time in stations as Asturias of Barcelona. However the same does not count for stations such as Madrid or Valencia. We did find clear seasonality when looking at the plots in **appendix x** of all weather stations.

3. Methodology

- **LMP model**
- **Logit/probit**
- **Logit/probit met lags**
- **Gam**
- **Validatie**
- **Overige dingetjes**

3.1 Choice of models

This study models extreme precipitation via exceedance probabilities rather than rainfall amounts. Precipitation regimes differ substantially across locations as observed in the descriptive statistics, making

fixed thresholds or level based modelling poorly comparable across stations. Exceedance indicators based on station-specific wet-day percentiles adapt automatically to local climate conditions: an exceedance always represents a comparable upper-tail event, regardless of whether a station is generally wet or dry. As a result, this approach provides a stable and interpretable probability target for detecting changes in extreme-event risk over time, rather than changes in average precipitation levels (Katz et al., 2002).

Several alternative econometric approaches were considered but not chosen given the study goals and sample constraints. Linear Probability Models are simple but can yield invalid probabilities and are heteroskedastic by construction (Wooldridge, 2010). Standard Logit/Probit GLMs ensure bounded probabilities, but produce linear trend/seasonal structure, which is restrictive when exceedance risk evolves nonlinearly over time (McCullagh & Nelder, 1989). The Extreme Value Theorem is well suited for marginal tail modelling, but becomes less practical when the objective is time-varying exceedance probabilities and joint exceedances across stations (Coles, 2001). Copula models offer a general dependence framework, but tail dependence is fragile in our sample size and chosen threshold, reducing stability for joint modelling (Genest & Favre, 2007).

Given these tradeoffs, this study uses a Generalized Additive Model (GAM), which allows for non-linear modelling of seasonality and long-term trends, while remaining feasible for both station-level and joint exceedance analysis. Specifically, this research uses a station specific daily GAM, and also a GAM for modelling joint exceedances within the same week.

3.2 Seasonal modelling

Seasonality in precipitation is non-linear, non-sinusoidal and potentially asymmetric. Therefore, it must be modelled in a befitting manner. Underwood (2009) states that Fourier terms or splines can be used to represent seasonality. Fourier terms represent seasonality by using k sine and cosine functions with fixed frequencies, requiring ad hoc choosing of k. Cyclic splines model seasonality smoother and in a data-driven manner.

This research compares a parametric Fourier representation with differing harmonic orders against a cyclic spline specification in table 2. The results show that cyclic splines offer a lower AIC score with comparable effective degrees of freedom. Therefore this research uses cyclic splines to model seasonality.

3.3 Generalized Additive Model (GAM)

In this research, a time-varying exceedance probability needs to be modelled while allowing for non-linear seasonal and long-term patterns. The Generalised Additive Model, GAM, is suitable for this goal. GAMs are an extension of Generalised Linear Models (GLMs), in which some of the terms in the model are replaced by non-linear functions. The underlying data affects the shape of the smooth function

(Underwood, 2009). This suits the precipitation data, where long-term trends and seasonal effects are rarely linear and may evolve.

As described in the data section, the GAM model will use the wet days and the days of extreme precipitation. Then the model will use the binary variables.

The non-linear relationships are modelled using penalised regression splines. In this research, two different types of spines are used: Thin Plate Regression Splines and the Cyclic Cubic regression splines. The thin plate regression splines are used for the time trend. These provide an approximation of smooth relationships without the need for manual knot selection. The Cyclic Cubic regression splines are used for the seasonal component, the day of the year. The splines construct a flexible, smooth curve by joining together multiple simpler polynomial segments at specific points, allowing the model to fit non-linear data patterns (Underwood, 2009).

The splines are controlled by a smoothing parameter, which decides how "stiff" the fitted functions are. Finding the optimal balance is crucial: If this parameter is too low, the model tends to overfit the data by tracking daily noise; if the parameter is too high, the resulting curve becomes too rigid, leading to underfitting. In this research, the smoothing parameters are estimated using Restricted Maximum Likelihood (REML).

While choosing the parameter with the lowest Akaike Information Criterion (AIC) or Generalized Cross Validation (GCV) are other common methods for parameter selection, REML is preferred for this research. As demonstrated, REML treats the smoothing penalty as a variance component. This approach provides a more pronounced optimum for the parameters and it is significantly more robust against occasional severe undersmoothing failures. In contrast, AIC and GCV will be more sensitive to undersmoothing failures because it does not penalize overfitting as much (Wood, 2011).

Because the data in this research are binary, selecting a robust criterion of importance. In such cases, the undersmoothing failures associated with AIC commonly produce spuriously wiggly functions. (Wood,2011)

3.3.2 Baseline station level GAM

The baseline model focuses on structural components only

$$\eta_{s,t}^{base} = \alpha_s + s_{season}(d_t) + s_{trend}(t)$$

Where seasonality is modelled using a cyclic cubic regression spline in day-of-year d_t, and long term evolution is captured by a smooth function of time *t* (days since start of sample).

3.3.3 Extended station level GAM

To assess robustness and improve short-term predictive performance, extended model specifications include covariates:

$$\eta_{s,t}^{ext} = \alpha_s + s_{season}(d_t) + s_{trend}(t) + \beta_1 Y_{s,t-1} + \beta_2 NAO_t + s_{int}(d_t, NAO_t)$$

First, a one-day lag of the exceedance indicator, $Y_{s,t-1}$ is included to account for clustering in extreme precipitation events. Extreme rainfall often occurs in multi-day storm systems, implying serial dependence in exceedance probabilities. Including a lag term allows the model to capture this persistence and improves short-term predictive performance. Second, large-scale atmospheric circulation is incorporated through the North Atlantic Oscillation (NAO) index, which influences precipitation variability over the Iberian Peninsula in a seasonally heterogeneous manner (Trigo et al., 2002; Burt & Howden, 2013; Vicente-Serrano et al., 2011). To capture this heterogeneity, the NAO index is interacted with the seasonal component, allowing for circulation-driven variation without affecting long-term trend estimation.

All models are estimated using the penalized likelihood with smoothing parameters selected via REML, implemented via the R-studio mgcv package.

3.3.5 Key Assumptions of the GAM framework

GAM frameworks assume an exponential-family outcome variable, a correctly specified link and mean-variance relationship, additive smooth covariate effects, and conditional independence of our observations (McCullagh & Nelder, 1989). Our Bernoulli model with a logit link satisfies the distributional and variance assumptions by construction, while smooth seasonality and trends are modelled; conditional independence may be imperfect due to temporal clustering, but is partly mitigated by including the lagged variable.

3.4 Joint Exceedance indicators

For this model, we augment the GAM in order to model the probability of joint exceedances occurring over time. Let $Y_w^{(k)} = 1\{\sum_{s=1}^{S} Y_{s,w} \geq k\}$, where $Y_{s,w} = 1$ if stations experienced at least one daily exceedance during week *w*. We aggregate weeks into ISO weeks in order to achieve this. In our research we use k=2 and k=3, meaning for the former that in a given week $Y_w^{(k)} = 1$ means that at least 2 stations

experienced an exceedance. Conditional on covariates, $Y_w^{(k)}$ follows a Bernoulli distribution with success probability $p_w^{(k)}$. The GAM is here also specified with a logit link function such that

$$logit(p_w^{(k)}) = \eta_{k,w}$$

In its base form, the model only includes structural components

$\eta_w^{(k),base} = \alpha^{(k)} + s_{season}(d_t) + s_{trend}(t)$, and in its extended form the model is specified as

$$\eta_w^{(k),extended} = a^{(k)} + s_{season}(d_t) + s_{trend}(t) + \beta_1 Y_{w-1} + \beta_2 NAO_w + s_{int}(d_t, NAO_t)$$

3.5 Validation testing

The validation procedure uses a temporal cross-validation scheme (as detailed in Section 3.4), ensuring that models are evaluated on future data not seen during training. For the validation of the GAM there will be made use of three popular metrics of evaluating probabilistic classifiers: the Brier Score, Logarithmic Loss (LL), and the Area Under the Receiver Operating Characteristic Curve (AUROC) (Decroos, T., & Davis, J. ,2019).

3.5.1 Brier score

This score is a measure of accuracy of probabilistic predictions. it is essentially the mean squared error between the prediction and the labels , it can only be minimized by reporting the true class distribution. The Brier score has the following formula;

$$BS = \frac{1}{N}\sum_{i}^{N}(p_i - y_i)^2$$

Where N denotes the number of days in the dataset,p the probability that was predicted for that specific day and y is the label of the specific day. (Decroos, T., & Davis, J. ,2019).

3.5.2 Logarithmic Loss

This method is another measure of accuracy of the probabilistic prediction, the difference between this measure and the Brier score is that the Logarithmic Loss weights the individual prediction errors. The formula is defined as;

$$LL = \frac{1}{N}\sum_{i}^{N} y_i \log p_i + (1 - y_i)\log(1 - p_i)$$

Where N, p and y have the same definition as in the formula of the Brier score. (Decroos, T., & Davis, J. ,2019).

3.5.3 Area Under the Receiver Operating Characteristic Curve

The AUROC is a measure that indicates how well a model indicates a positive from a negative case. In the article of Decroos and Davis it states that it will answer the following intuitively question, “Given a

positive example and a negative example, how likely is it that our classifier will correctly rank the positive example ahead of the negative example?" (Decroos, T., & Davis, J. ,2019). This can be interpreted as the ranking over probability, a downfall to this validation is that a model can be poorly calibrated, meaning it will predict probabilities that would not match reality, but yet AUROC score will still be high.(Decroos, T., & Davis, J. ,2019)

3.6 Mann-Kendall trend test

As a preliminary nonparametric diagnostic, Mann-Kendall tests were applied to station-level exceedance series (Appendix ..). Except for Vigo, no significant monotonic trends were detected. Given the sensitivity of such tests to serial dependence, these results are treated as contextual diagnostics rather than inferential evidence, motivating the use of flexible GAM specifications.

Dit is even een chat tekst:

Basisdimensionering en modelopbouw
De analyse is uitgevoerd met binomiale generalized additive models (GAMs). De basisdimensie kkk bepaalt daarbij slechts de maximale flexibiliteit van een smooth; de effectieve complexiteit wordt gecontroleerd via penalization (Wood, 2017). Om te voorkomen dat structurele patronen in de residuen worden geforceerd, is de adequaatheid van kkk voorafgaand aan verdere diagnostiek beoordeeld met de k-index uit gam.check.
Voor elk model zijn basisdimensies iteratief verhoogd totdat geen consistente aanwijzingen voor undersmoothing meer aanwezig waren. In het baseline-model gaf de k-index een signaal voor resterende structuur, met name voor de langetermijntrend. De effectieve vrijheidsgraden voor s(time)s(\text{time})s(time) bleven echter zeer laag (edf ≈ 1), wat erop wijst dat dit signaal niet werd veroorzaakt door een te restrictieve basisdimensie, maar door modelmisspecificatie. Dit is consistent met eerdere bevindingen dat de k-index gevoelig kan zijn voor onbegrepen seriële afhankelijkheid.
Daarom is de gemiddelde structuur uitgebreid met een persistentieterm (lag1\text{lag1}lag1), die aangeeft of op de vorige dag een exceedance optrad. Deze toevoeging elimineerde het k-index-signaal en reduceerde residuele autocorrelatie substantieel. Vervolgens is de North Atlantic Oscillation (NAO) toegevoegd als grootschalige circulatie-indicator. In het lag+NAO-model vertoonden residuen geen duidelijke resterende seriële structuur.
Een expliciete AR(1)-correctie is aanvullend onderzocht met bam als robuustheidscheck, maar leverde vrijwel identieke fits en voorspellingen op. Seriële afhankelijkheid werd daarom als voldoende gemodelleerd via de gemiddelde structuur. De uiteindelijke basisdimensies (tijd: k=30–40k=30\text{–}40k=30–40; seizoen: k=18–20k=18\text{–}20k=18–20) zijn behouden.

Concurvity diagnostics indicated no severe dependence among smooth terms; detailed results are provided in Appendix X.

Validatie

De voorspelprestatie is geëvalueerd met blocked time-series cross-validation (drie tijdsblokken). Over de folds heen behaalde het lag+NAO-model de laagste gemiddelde LogLoss en een duidelijke verbetering in AUC ten opzichte van zowel het baseline-model als climatologie. Een seizoensafhankelijke NAO-interactie leverde slechts marginale extra winst op en werd daarom niet als voorkeursmodel geselecteerd.

Model	Term	k′	edf	k-index	p
Baseline	s(time)	29	1.0	0.85	0.005
Baseline	s(doy)	18	6.1	0.86	0.007
Lag	s(time)	29	1.0	0.92	0.99
Lag + NAO	s(time)	39	1.0	0.91	0.18

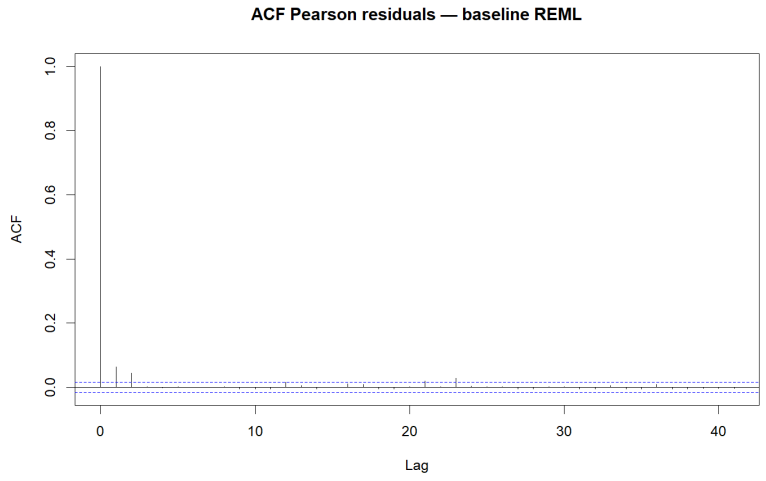

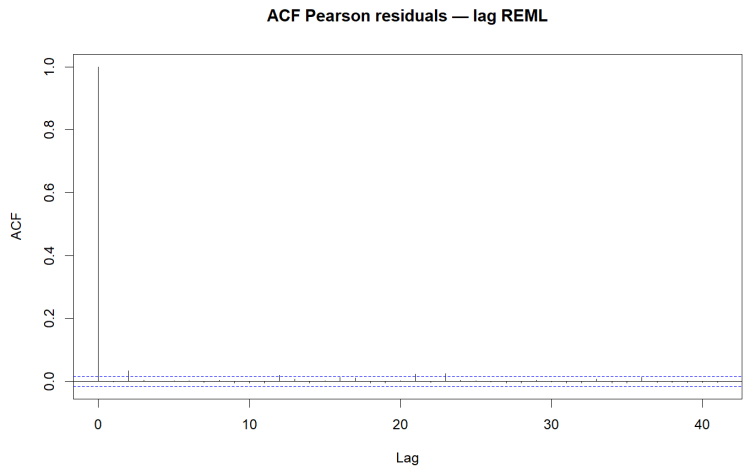

Hier zie je dat na de toevoeging van de lag de autocorrelation eruit gaat. Dan verdwijnt ook de significantie van de k in de tabel zonder dat hij is opgehoogd.

https://webhomes.maths.ed.ac.uk/~swood34/test-gam.pdf

https://pmc-ncbi-nlm-nih-gov.eur.idm.oclc.org/articles/PMC6542350/pdf/peerj-07-6876.pdf

Zijn papers die kunnen helpen.

Model	Mean LogLoss	Mean Brier	Mean AUC
lag + NAO	**0.0238**	0.00371	0.690
lag + NAO × season	0.0239	0.00371	**0.693**
lag	0.0242	0.00371	0.640
baseline	0.0244	0.00370	0.639
climatology	0.0247	0.00370	0.500

Dit is van alicante (die drie folds weer)

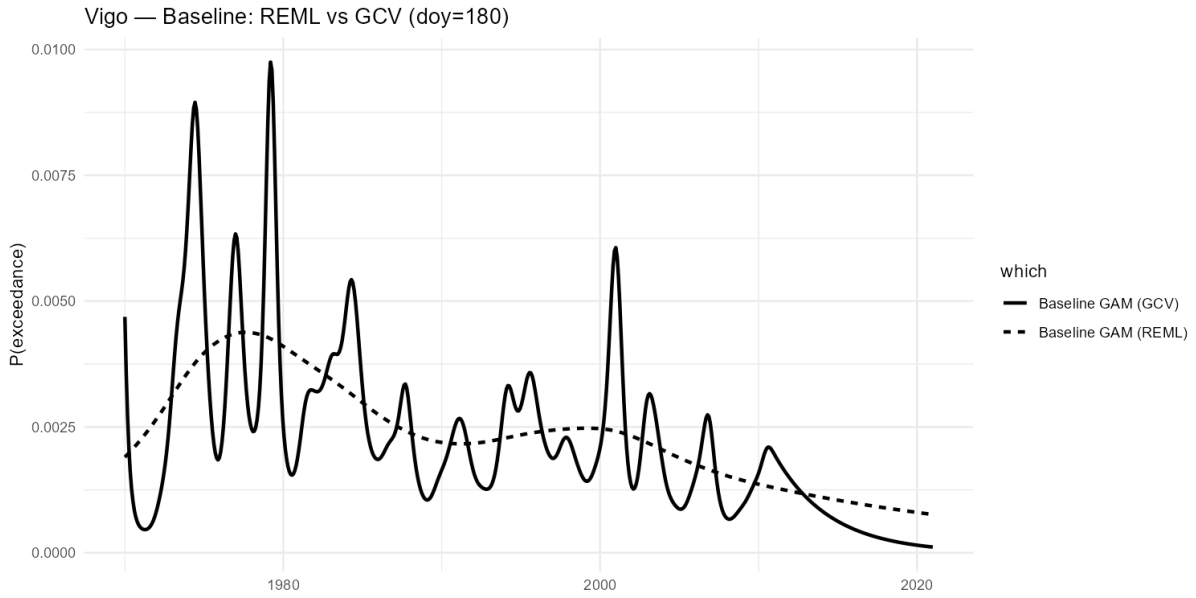

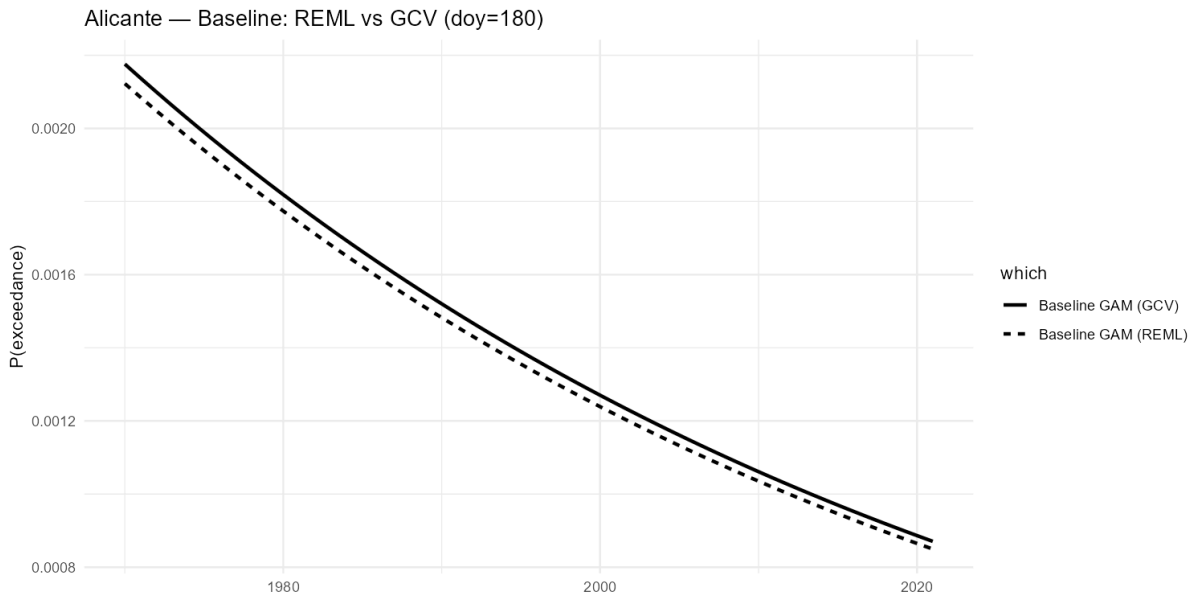

4. Results

4.1 Individual station-level exceedance probability (Alicante)

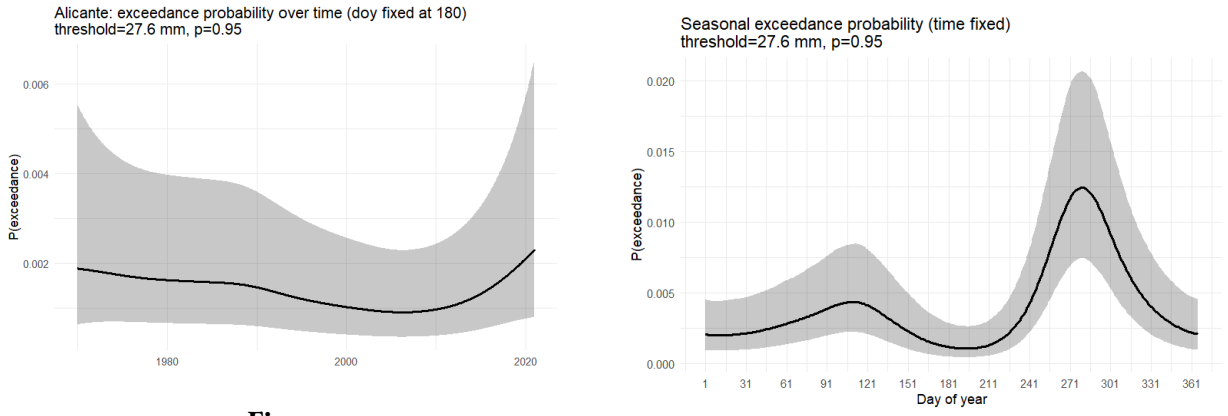

Figure x

Figure X shows the estimated probability of exceeding the station-specific 95th wet-day percentile for Alicante from the baseline GAM, with seasonal effects fixed at their median value in order to isolate the long-term component of exceedance risk. Exceedance risk exhibits pronounced seasonality, with a clear peak in late summer and autumn. This seasonal concentration aligns with the period in which intense convective rainfall and DANA-related events are most frequently observed along the Spanish Mediterranean coast.

The estimated long-term component of exceedance risk is non-monotonic, declining during the early part of the sample period and increasing modestly in more recent decades. However, the associated confidence band remains wide throughout the sample, indicating substantial uncertainty and providing no clear evidence of a persistent upward trend in extreme precipitation risk at the station level.

Results for additional stations and extended model, covering both Mediterranean and Atlantic climate regimes, display similar non-monotonic behaviour with varying degrees of seasonal concentration and are reported in Appendix X.

4.3 Joint exceedance GAM

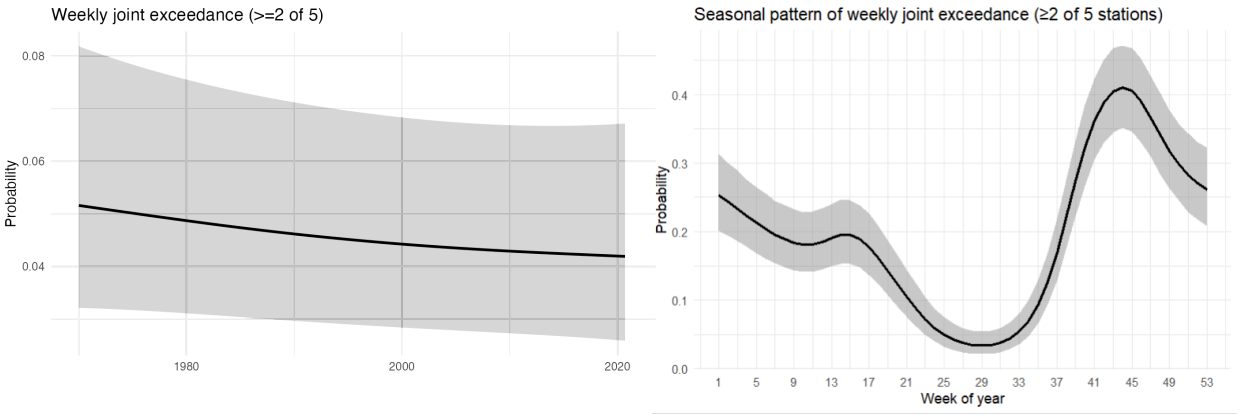

Figure X presents the estimated probability that at least two stations experience an extreme precipitation exceedance within the same week, based on the baseline joint exceedance GAM. The left panel shows the long-term component evaluated at median seasonal conditions, while the right panel shows the seasonal component.

Joint exceedance probabilities exhibit strong seasonal variation, with higher probabilities during autumn and winter months. The estimated long-term component remains broadly stable over the sample period and does not display a monotonic trend. Results for the stricter $k \geq 3$ definition and the extended model are qualitatively similar and reported in Appendix X.

4.4 Diversification diagnostics

Appendix 6 reports weekly joint exceedance probabilities for selected station pairs based on the baseline joint exceedance model. The table highlights pairs with the highest and lowest probabilities of joint exceedance. Pairs with the highest joint exceedance probabilities, such as Vigo and Asturias with 152 joint exceedances, predominantly consist of stations within the same climatic region, while pairs with the lowest probabilities typically involve stations from different regions. An example of this is Vigo-Alicante with only 13 exceedances

→ heel evt nog link naar case

4.4 Station level GAMs validation

model	mean_brier	mean_logloss	mean_auc	rank_logloss	rank_brier	rank_auc
base+lag+naoSeason	0.008500	0.04675	0.7022	1	1	1
base	0.008575	0.04856	0.6599	6	5	6
benchmark	0.008559	0.04878	0.5000	7	4	7

Table 5

Table 5 reports out-of-sample predictive performance for station-level exceedance models based on time-based cross-validation. Reported scores represent the mean across three non-overlapping temporal folds.

The baseline GAM clearly outperforms the benchmark across all metrics, indicating substantial predictive skill. The extended specification yields modest but consistent improvements in Brier score, log loss, and AUC relative to the baseline model. These improvements do not materially change the estimated exceedance probability patterns, supporting the use of the baseline model for interpretation. / Estimated exceedance probabilities are very similar across specifications.

4.5 Joint exceedance GAMs validation

model	mean_brier	mean_logloss	mean_auc	rank_brier	rank_logloss	rank_auc	rank_total
base+lag+naoSeason	0.1778	0.5300	0.7188	1	1	1	1
base	0.1820	0.5390	0.6999	6	6	6	6
benchmark	0.2012	0.5921	0.5000	7	7	7	7

Table 6

Table 6 reports out-of-sample validation results for joint exceedance models under the k≥2 specification, averaged across three temporal cross-validation folds.

Relative to the benchmark, the baseline joint exceedance model achieves substantially better predictive performance. The extended specification provides additional, moderate improvements across all validation metrics. Estimated joint exceedance probabilities remain similar across model specifications.
→ calibration plot?

5. Discussion

- Een idee eerder verschillende stations (obv waar) in die paren top 3 beste/slechste paren verklaren → linken met klimaat waar stations vandaan komen (dit moet dan ook in data zijn beschreven kort)

Kort over nao/extended model:
While the inclusion of NAO improves predictive performance, it does not materially alter estimated exceedance trends, consistent with its role as a driver of seasonal variability rather than long-term change.

5.1 Station-level exceedance behaviour

The absence of a clear monotonic trend in station-level exceedance probabilities for Alicante, as estimated by the baseline model, is consistent with earlier findings for Mediterranean Spain, where extreme precipitation is characterized by strong seasonality and pronounced regional heterogeneity rather than uniform long-term change (Vicente-Serrano et al., 2011; Senent-Aparicio et al., 2023). In such settings, station-level variability is largely driven by episodic convective events and synoptic disturbances, which complicates robust trend detection.

From this perspective, the severe impacts observed during the September 2019 DANA can be interpreted as being consistent with extreme precipitation occurring during a climatologically high-risk season along the Mediterranean coast, rather than necessarily reflecting a structural shift in long-term exceedance risk at this station. This interpretation suggests that seasonal concentration plays an important role in shaping extreme precipitation risk for Alicante, motivating the subsequent focus on joint exceedance behaviour.

5.2 Joint exceedance risk and spatial dependence

The joint exceedance results underscore that changes in marginal extreme precipitation risk do not automatically translate into stronger spatial clustering of extremes. In line with the joint-extremes literature, spatial tail behaviour appears to be governed primarily by episodic large-scale atmospheric configurations rather than by gradual long-term change (Katz et al., 2002; Cooley et al., 2006). This distinction is particularly relevant in climatically heterogeneous regions such as Spain.

Seasonal modulation of joint exceedance risk reflects periods in which synoptic conditions allow extremes to occur simultaneously across locations, rather than a simple aggregation of station-level seasonality. The September 2019 DANA event - during which exceedances occurred concurrently at Alicante, Valencia and Barcelona - can therefore be interpreted as a realization of seasonally elevated joint risk along the Mediterranean coast, rather than as evidence of a structural increase in spatial dependence. This interpretation is consistent with previous findings for Southern Europe, which emphasize heterogeneous and episodic drivers of extreme precipitation (Vicente-Serrano et al., 2011; Senent-Aparicio et al., 2023).

Results for the stricter $k \geq 3$ definition, reported in Appendix X, support this conclusion despite greater estimation uncertainty due to event rarity. Station-pair patterns further indicate that the strongest joint exceedance probabilities arise primarily among geographically and climatically similar stations, while combinations spanning different climate regimes exhibit greater diversification. This reinforces the view that spatial heterogeneity remains a key determinant of precipitation risk aggregation, with direct implications for geographic diversification in insurance portfolios (Martínez-Salgueiro & Tarrazon-Rodon, 2021).

5.3 Diversification potential across station pairs

5.4 Model performance and predictive implications

5.5 Limitations and implications

6. Conclusion

This research investigated the temporal trends and spatial correlations of tail-end precipitation events in Spain (1970–2020) to inform risk assessment for parametric insurance. By employing a GAM with station-specific thresholds, by doing this the focus shifted from modeling and analyzing average rainfall to the cases where extreme events occurred. The analyzation of these extreme events will be done with answering the following sub questions:

> *What is the probability that precipitation crosses the 95th wet day percentile at any given day in the year for Spanish weather stations, and is there evidence of this probability changing over time?*
> *Is there evidence of the daily probability of spatially correlated joint precipitation exceedances above the 95th percentile across Spain changing over time?*

From the results the above question can be answered. The analysis reveals that the probability of exceeding the 95th wet-day percentile is highly seasonal, peaking in autumn across all stations. While the NAO suggests a general drying trend in Southern Europe due to positive NAO phases, our station-level GAMs show a more nuanced reality. Stations like Asturias and Vigo show a significant long-term decrease in total precipitation, yet recent years exhibit an upwards trend in exceedance probabilities. This suggests that while it may rain less frequently, the intensity of extreme events remains stable or even increases in specific regions. Spatially Correlated Joint Exceedances Regarding the risk of mass-payout events, our joint exceedance GAM (for $k \geq 2$ and $k \geq 3$ stations) indicates a slight downward slope over time. There is no evidence of a significant increase in the probability of synchronized extreme events across the Spanish peninsula. From an underwriting perspective, this suggests that the systemic risk of simultaneous claims across these specific geographies has not worsened over the last 50 years.

For further research we would recommend to research which of the weather station pairs exhibit the weakest/strongest diversification and how this is related to climate regimes. Waarom is dit een interessante vraag?

References

Allen, M. R., & Ingram, W. J. (2002). "Constraints on future changes in climate and the hydrologic cycle." Nature, 419(6903), 224-232

Bracken, C., Rajagopalan, B., & Cheng, L. (2016). Spatial dependence of precipitation extremes in Europe. Journal of Climate, 29(19), 6905–6920.

Burt, T. P., & Howden, N. J. K. (2013). North Atlantic Oscillation amplifies orographic precipitation and river flow in upland Britain. *Water Resources Research*, *49*(6), 3504–3515. https://doi.org/10.1002/wrcr.20297

Climate Prediction Center - Teleconnections: North Atlantic oscillation. (2026). https://www.cpc.ncep.noaa.gov/products/precip/CWlink/pna/nao.shtml

Donat, M. G., et al. (2016). More extreme precipitation in the world's dry and wet regions. Nature Climate Change, 6, 508–513

Hamed, K. H., & Rao, A. R. (1998). A modified Mann-Kendall trend test for autocorrelated data. Journal Of Hydrology, 204(1–4), 182–196. https://doi.org/10.1016/s0022-1694(97)00125-x

IPCC. (2021). AR6 Working Group I – The Physical Science Basis. Cambridge University Press.

Kendall, M.G., 1955. Rank Correlation Methods. Griffin, London.

Mann, H.B., 1945. Nonparametric tests against trend, Econometrica, 13, 245-259.

McCullagh, P., & Nelder, J. A. (1989). *Generalized Linear Models, Second Edition*. CRC Press.

Mukherjee, S. (2025, 17 September). *Linear Probability Model: Definition, Examples & Limitations*. https://www.digitalocean.com/community/conceptual-articles/linear-probability-model

Schmelzer, C. H. M. A. A. G. A. M. (2025, 17 October). *11.2 Probit and Logit Regression | Introduction to Econometrics with R*. https://www.econometrics-with-r.org/11.2-palr.html

Spanjers, B., Beutner, E., Coumou, D., & Schaumburg, J. (2025). Increased persistence of warm and wet winter weather in recent decades in north-western Europe. Communications Earth & Environment, 6(1), 760.

Trigo, R. M., et al. (2002). Influence of the NAO on European precipitation. International Journal of Climatology, 22(12), 1385–1398.

Urrea Méndez, D., & del Jesus, M. (2023). Estimating extreme monthly rainfall for Spain using non-stationary techniques. Hydrological Sciences Journal, 68(7), 903–919. https://doi.org/10.1080/02626667.2023.2193294

Decroos, T., & Davis, J. (2019). Interpretable Prediction of Goals in Soccer.

Appendix

Appendix 1: QQ plot of the daily precipitation in Asturias

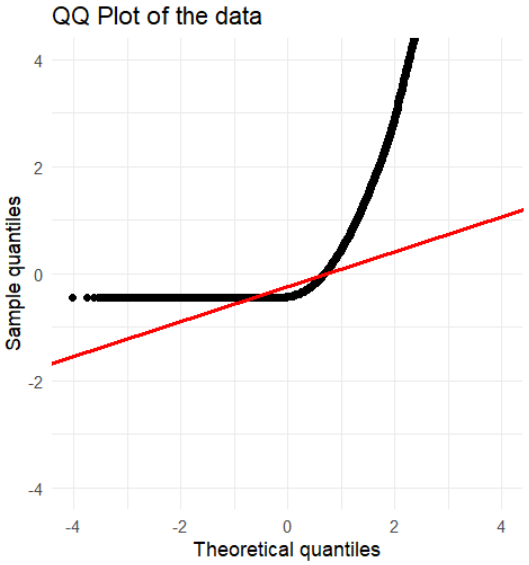

Appendix 2: Trends and seasonality in data of remaining 6 weather stations

<u>Alicante:</u>

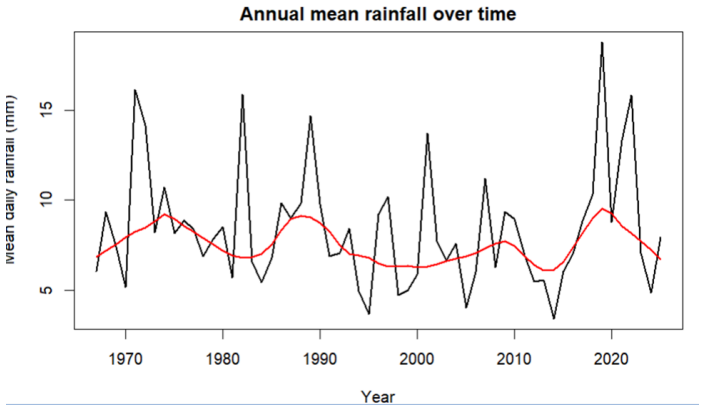

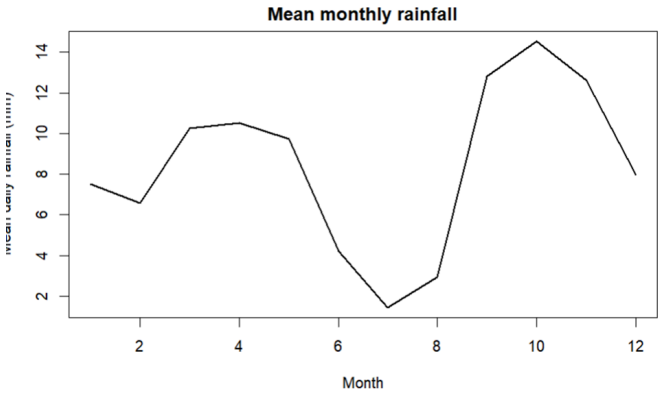

Vigo

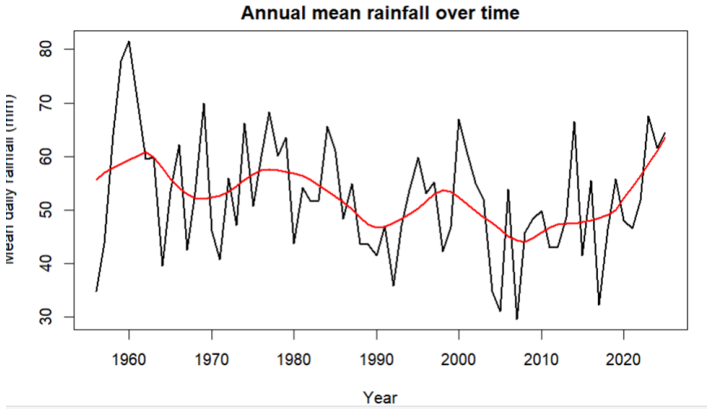

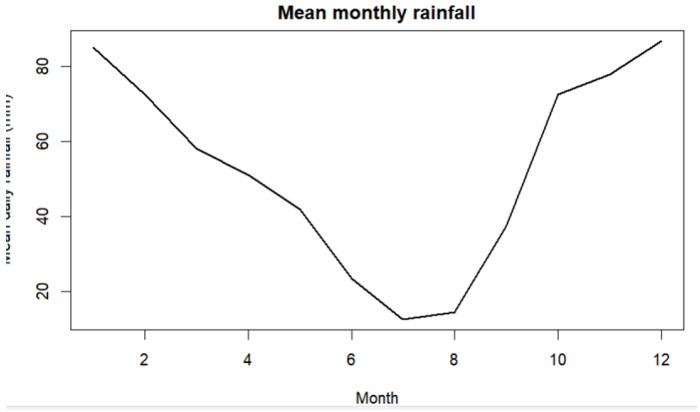

Barcelona

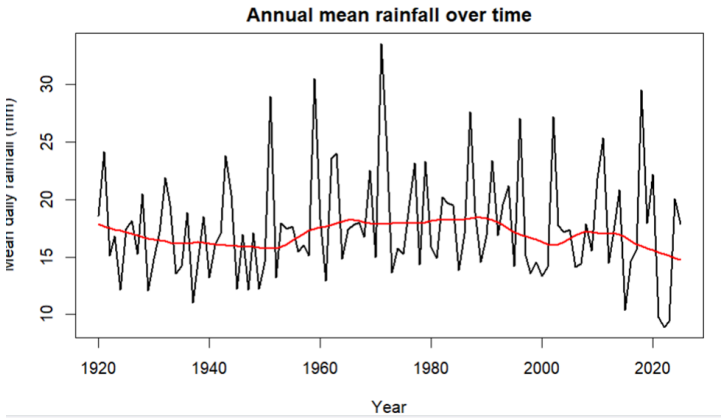

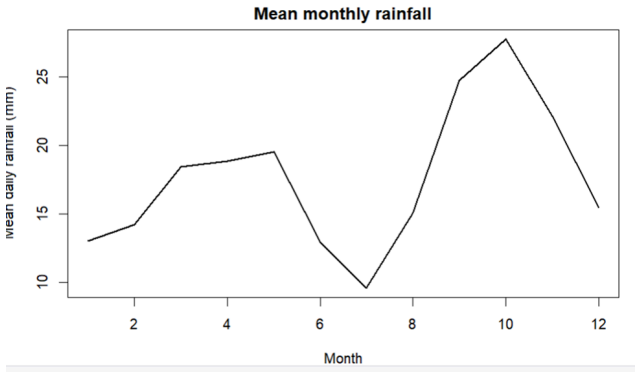

Madrid:

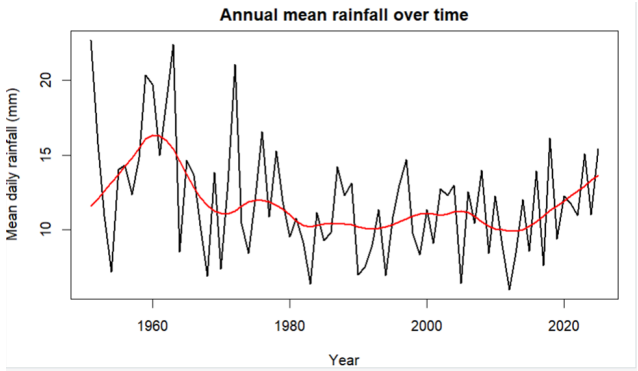

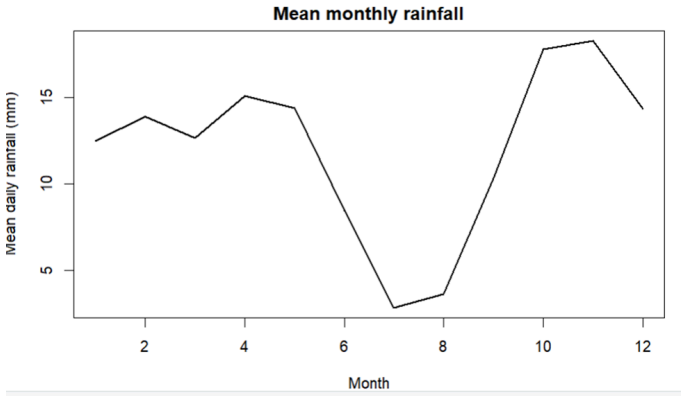

Valencia:

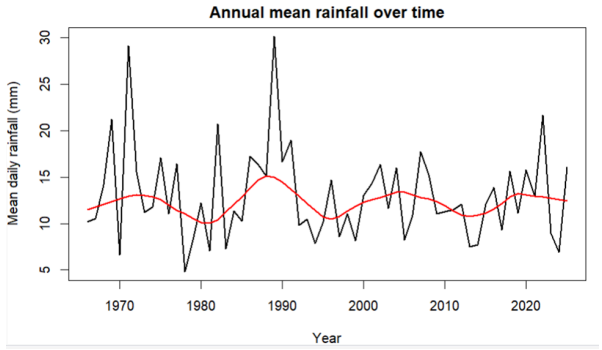

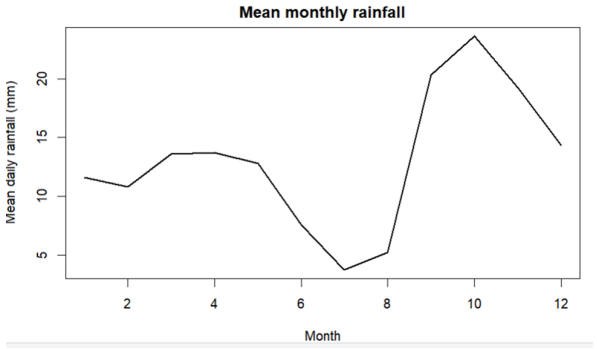

Sevilla:

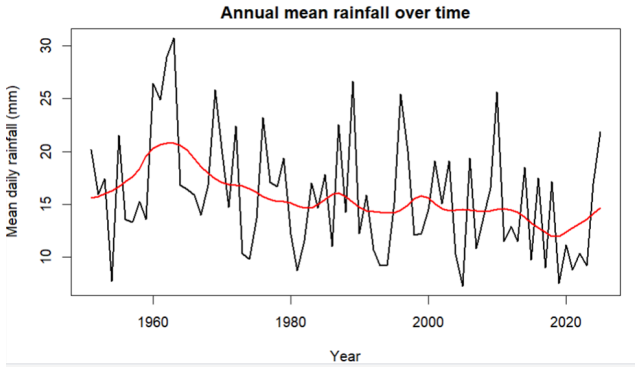

Appendix: Not chosen models.

Several alternative econometric approaches were considered but not chosen given the study goals and sample constraints. The Extreme Value Theorem is well suited for marginal tail modelling, but becomes less practical when the objective is time-varying exceedance probabilities and joint exceedances across stations (Coles, 2001). Copula models offer a general dependence framework, but tail dependence is fragile in our sample size and chosen threshold, reducing stability for joint modelling (Genest & Favre, 2007).

Appendix 3: Fourier Terms vs Cyclic Cubic Splines

station	model_name	season_type	K_fourier	AIC	delta_AIC	edf_time	edf_season	n_coef
Madrid	cyclic_spline	cyclic_spline	NA	1579.2705211983	3.76991144371891	2.30815633969537	5.55563879707808	49
Madrid	fourier_K1	fourier	1	1591.74404372005	16.2434339654696	2.3021777040885	NA	33
Madrid	fourier_K2	fourier	2	1581.90214366039	6.40153390581031	2.3166122284336	NA	35
Madrid	fourier_K3	fourier	3	1575.50060975458	0	2.30496564386212	NA	37

Madrid	fourier_K4	fourier	4	1577.05404771728	1.55343796270222	2.30952426340049	NA	39
Madrid	fourier_K5	fourier	5	1579.65085481329	4.15024505871452	2.30562858922425	NA	41
Madrid	fourier_K6	fourier	6	1577.40263262059	1.90202286601311	2.30150148189243	NA	43
Barcelona	cyclic_spline	cyclic_spline	NA	1598.24994213905	1.42361478196426	1.00089163060694	5.36594242627306	49
Barcelona	fourier_K1	fourier	1	1617.48967710215	20.6633497450737	1.00086598310357	NA	33
Barcelona	fourier_K2	fourier	2	1596.82632735708	0	1.00088635738436	NA	35
Barcelona	fourier_K3	fourier	3	1598.13614131303	1.30981395594563	1.00090321640948	NA	37
Barcelona	fourier_K4	fourier	4	1600.15792484914	3.33159749206175	1.00090001291683	NA	39
Barcelona	fourier_K5	fourier	5	1603.21050496552	6.38417760843777	1.00090317174828	NA	41
Barcelona	fourier_K6	fourier	6	1598.04103532877	1.21470797169309	1.00091197738111	NA	43
Asturias	cyclic_spline	cyclic_spline	NA	3091.68409211231	1.71924528982072	3.34576525740439	5.12865338495282	49
Asturias	fourier_K1	fourier	1	3104.83686015667	14.8720133341858	3.36018577394201	NA	33
Asturias	fourier_K2	fourier	2	3089.96484682249	0	3.33203046465801	NA	35
Asturias	fourier_K3	fourier	3	3090.13137164618	0.16652482369681	3.34352603000123	NA	37
Asturias	fourier_K4	fourier	4	3093.11263381857	3.14778699608451	3.3530157842287	NA	39
Asturias	fourier_K5	fourier	5	3095.76310616842	5.79825934592918	3.35749445353817	NA	41
Asturias	fourier_K6	fourier	6	3096.88662208432	6.92177526183104	3.34856699360249	NA	43
Sevilla	cyclic_spline	cyclic_spline	NA	1405.36429082162	1.77112916942519	1.87522567398583	4.66342809336484	49
Sevilla	fourier_K1	fourier	1	1407.31489010369	3.72172845149612	1.88079015453904	NA	33

Sevilla	fourier_K2	fourier	2	1404.0867650242	0.49360337200710 1	1.8725537635708 2	NA	35
Sevilla	fourier_K3	fourier	3	1403.5931616521 9	0	1.8738511937923 7	NA	37
Sevilla	fourier_K4	fourier	4	1406.6139858579 7	3.02082420577563	1.8726365900732 7	NA	39
Sevilla	fourier_K5	fourier	5	1409.1887537537 2	5.59559210153202	1.8781566188545 3	NA	41
Sevilla	fourier_K6	fourier	6	1407.8084998266	4.21533817440991	1.8742512771207 8	NA	43
Vigo	cyclic_spline	cyclic_spline	NA	2889.0773541907 8	3.14068981868741	1.0023643786448 6	6.0304592486027 8	49
Vigo	fourier_K1	fourier	1	2897.0062483917 4	11.0695840196408	1.0024579161375 3	NA	33
Vigo	fourier_K2	fourier	2	2892.1110961459 9	6.17443177389305	1.0016721187997 6	NA	35
Vigo	fourier_K3	fourier	3	2885.9366643721	0	1.0017980889060 2	NA	37
Vigo	fourier_K4	fourier	4	2886.2767540099 9	0.34008963789756 3	1.0026096376056 5	NA	39
Vigo	fourier_K5	fourier	5	2889.4754756699 5	3.53881129785714	1.0024534575613 9	NA	41
Vigo	fourier_K6	fourier	6	2891.0477587593 5	5.11109438724998	1.0014628878667 8	NA	43
Valencia	cyclic_spline	cyclic_spline	NA	1208.0580638074 6	2.42242629325597	1.0006667710450 1	3.7744512916155 8	49
Valencia	fourier_K1	fourier	1	1211.2229304174 2	5.58729290321548	1.0006672037565	NA	33
Valencia	fourier_K2	fourier	2	1205.6356375142 1	0	1.0006691354225 6	NA	35
Valencia	fourier_K3	fourier	3	1208.8908388128 6	3.25520129865276	1.0006651278182	NA	37
Valencia	fourier_K4	fourier	4	1212.4762202254	6.84058271118806	1.0006648682014 2	NA	39
Valencia	fourier_K5	fourier	5	1215.1413575730 7	9.50572005886534	1.0006645649781 8	NA	41
Valencia	fourier_K6	fourier	6	1217.9572166487 4	12.3215791345372	1.0006606485713	NA	43

Alicante	cyclic_spline	cyclic_spline	NA	1009.7839838463 8	3.99573933512158	2.8730977713670 1	5.4851280273360 1	49
Alicante	fourier_K1	fourier	1	1030.7277657244 5	24.9395212131941	2.8008291358286 6	NA	33
Alicante	fourier_K2	fourier	2	1006.1698772049 9	0.3816326937349	2.8733217525704 8	NA	35
Alicante	fourier_K3	fourier	3	1005.7882445112 6	0	2.8905227395707 8	NA	37
Alicante	fourier_K4	fourier	4	1009.3223476058 3	3.53410309457001	2.8897844517027 9	NA	39
Alicante	fourier_K5	fourier	5	1012.8143270016 8	7.02608249041805	2.8930750461948 9	NA	41
Alicante	fourier_K6	fourier	6	1015.5591844984 5	9.77093998719442	2.8857014841015 9	NA	43

Appendix 3:

station	model	mean_AIC	mean_BIC	mean_logLik	mean_edf
alicante	base+lag+nao	616.973142978499	688.566723824697	-298.580290004496	9.08358672767194
alicante	base+lag+naoSeason	618.3265067537	697.675774523134	-298.206595908759	9.38504248063133
alicante	base+lag	622.705476021152	686.6409075526	-302.506721230335	7.98520511369406
alicante	base+nao	625.863912249456	691.268341045623	-303.884722485367	8.2991679587656
alicante	base+naoSeason	627.847247989089	705.611099004076	-303.187101022771	8.84600460874074
alicante	base	632.653946766233	690.460321964689	-308.331867095519	7.21560959705022
alicante	logit_lag1	642.247879307359	656.682752341113	-319.12393965368	0
alicante	logit_intercept	657.456477218648	664.67401710804	-327.728238609324	0
asturias	base+lag+naoSeason	1906.83657839476	2004.35097129573	-940.001559515789	11.0247727805115
asturias	base+lag	1913.03981065047	1980.32152618374	-947.2476492837	7.72660253913597
asturias	base+lag+nao	1913.97127238718	1988.08066326359	-946.776407583399	8.66516137358458
asturias	base+naoSeason	1919.42688064461	2013.75366453934	-946.741410654132	10.4724801110789
asturias	base	1927.08873135543	1990.16271241089	-954.856870844556	7.05186926990442
asturias	base+nao	1927.82422195616	1997.70810883328	-954.289592311271	7.99519006337932
asturias	logit_lag1	1930.3042701583	1944.80234816494	-963.152135079148	0
asturias	logit_intercept	1947.76985247899	1955.01899131318	-972.884926239496	0
barcelona	base+lag+naoSeason	1012.81631945506	1096.210204316	-494.950950173227	9.54536826954334

barcelona	base+lag	1013.67245708793	1071.0457861915	-498.97847676828	6.75697899939746
barcelona	base+lag+nao	1014.89766316762	1079.85300718921	-498.544673800231	7.79936836019594
barcelona	logit_lag1	1022.21312360329	1036.69734549624	-509.106561801644	0
barcelona	base+naoSeason	1027.54778892464	1107.59549650832	-502.780422220184	9.07729730918974
barcelona	base	1029.59976547606	1082.74783638017	-507.52687233529	6.14760276862973
barcelona	base+nao	1030.73830513954	1091.40599208661	-507.058203996666	7.19097677272153
barcelona	logit_intercept	1041.46257160444	1048.70478318613	-519.731285802219	0
madrid	base+naoSeason	957.948806649673	1051.65637782127	-466.156503222424	10.5013088321937
madrid	base+lag+naoSeason	959.527633674804	1060.1457133443	-465.990131777539	11.4577557882503
madrid	base+nao	966.053488485123	1037.51595015084	-473.265970875078	8.15651746352508
madrid	base+lag+nao	967.586248368405	1045.82956098451	-473.094754772082	9.09599815290161
madrid	base	969.694383096145	1036.08691379961	-475.778449399988	7.46147535945588
madrid	base+lag	971.216174716642	1044.19850591146	-475.629064018106	8.37940083880751
madrid	logit_intercept	986.027609222612	993.261724927673	-492.013804611306	0
madrid	logit_lag1	986.899976785505	1001.36800483435	-491.449988392753	0
sevilla	base+lag+naoSeason	826.874013963177	919.815838097274	-400.63741117757	11.0012303618397
sevilla	base+naoSeason	831.688959378587	919.849598852253	-403.698419528085	10.296852685879
sevilla	base+lag+nao	845.698386077009	904.307470462104	-414.787544146569	7.4881601013017
sevilla	base+nao	852.509746160965	905.041133849375	-419.029955781064	6.62319660207189
sevilla	base+lag	871.166233557401	921.16482440434	-428.707759568281	6.3812105997165
sevilla	base	881.509249351556	925.228768295833	-434.745625789743	5.49910039701339
sevilla	logit_lag1	905.582146487665	920.088050429697	-450.791073243832	0
sevilla	logit_intercept	920.501136530256	927.75418809586	-459.250568265128	0
valencia	base+lag+nao	725.923220522638	791.029308105026	-353.99643620241	7.73214702329208
valencia	base+lag+naoSeason	726.157287582751	795.10314345052	-353.589684977871	8.05446911397085
valencia	base+lag	729.866124514903	788.038900315572	-356.927128214855	6.75134247114499
valencia	logit_lag1	749.75603825509	764.215057595706	-372.878019127545	0
valencia	base+nao	760.376657246228	825.694447831918	-371.191873185888	7.44061430526249
valencia	base+naoSeason	760.633254755493	836.81231698827	-369.835589034188	8.38433070485976
valencia	base	764.80674478661	822.954181548111	-374.399290828669	6.44532369764363
valencia	logit_intercept	793.694247629856	800.923859340382	-395.847123814928	0
vigo	base+lag+nao	1766.78173400231	1862.51915949041	-870.321214379316	11.3530085358581

vigo	**base+lag+naoSeason**	**1767.64114740163**	**1871.09481463939**	**-869.66639896181**	**11.8171707877649**
vigo	**base+lag**	**1786.64050747032**	**1874.75444503388**	**-881.299827295847**	**10.4672511770061**
vigo	**base+nao**	**1794.04716713725**	**1885.58915751421**	**-884.529860955825**	**10.9356577347882**
vigo	**base+naoSeason**	**1794.98049699609**	**1895.54823132316**	**-883.739620999662**	**11.4382346433096**
vigo	**base**	**1817.83198859544**	**1901.51329639448**	**-897.504678873274**	**9.96136059533098**
vigo	**logit_lag1**	**1908.47819894019**	**1923.06058432286**	**-952.239099470095**	**0**
vigo	**logit_intercept**	**1964.31589583524**	**1971.60718425802**	**-981.157947917622**	**0**

Validation testing

model	mean_brier	mean_logloss	mean_auc	n_rows	n_auc	rank_logloss	rank_brier	rank_auc	rank_total
base+lag+naoSeason	0.00850104147500009	0.0468683791977245	0.700580435628983	21	21	1	1	1	1
base+lag+nao	0.00850484555060932	0.0470631412990019	0.689411749027827	21	21	2	2	2	2
base+lag	0.00851058513094063	0.0473902494147764	0.670874879441956	21	21	3	4	5	4
logit_lag1	0.00850490875441626	0.0476957230434661	0.534047349327783	21	21	4	3	7	4.66666666666667
base+naoSeason	0.00857909434226685	0.0481390727394024	0.688275356086143	21	21	5	8	3	5.33333333333333
base+nao	0.00858209296913031	0.0483445795236235	0.676145579918035	21	21	6	9	4	6.33333333333333
base	0.00857565632033782	0.0485979733897884	0.657591802298977	21	21	7	7	6	6.66666666666667
climatology	0.00856051008319376	0.0487802473988655	0.5	21	21	8	5	8.5	7.16666666666667
logit_intercept	0.00856051008322578	0.0487802474024608	0.5	21	21	9	6	8.5	7.83333333333333

Appendix 4: GAM predicted probabilities of threshold exceedance for each weather station

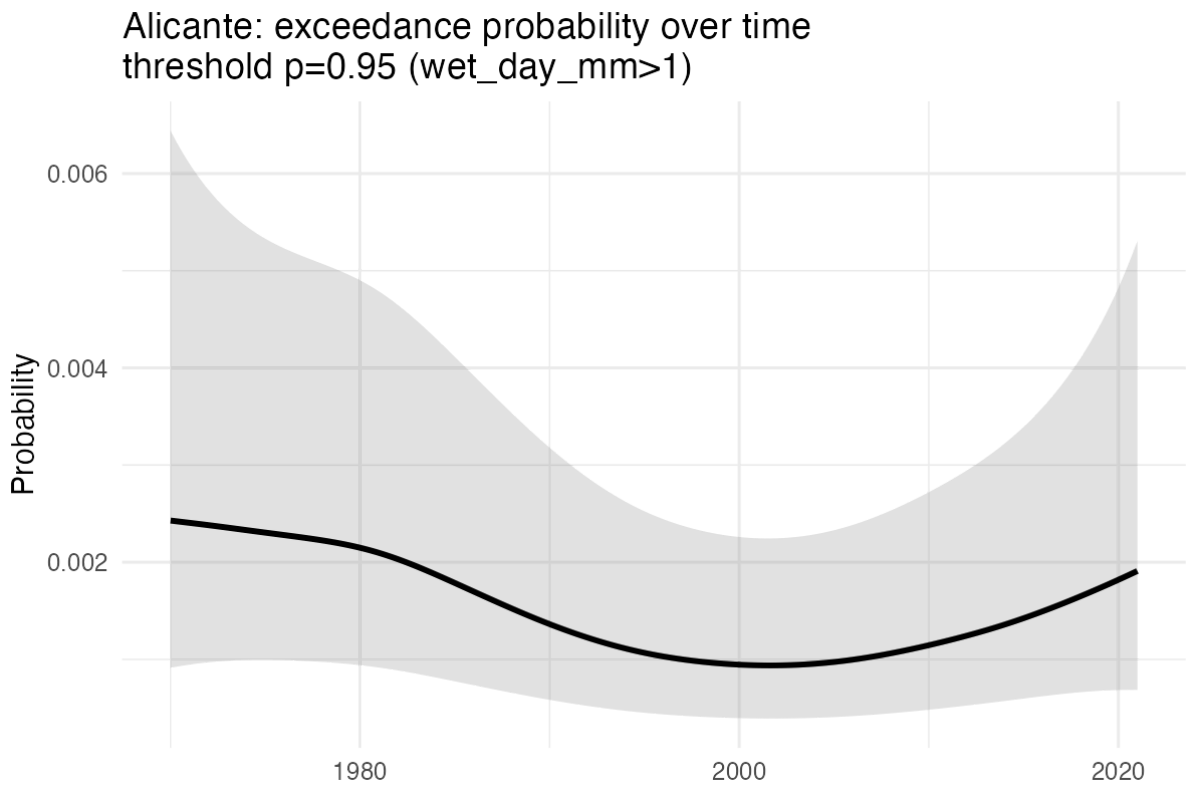
Alicante: exceedance probability over time
threshold p=0.95 (wet_day_mm>1)
Probability
0.006
0.004
0.002
1980
2000
2020

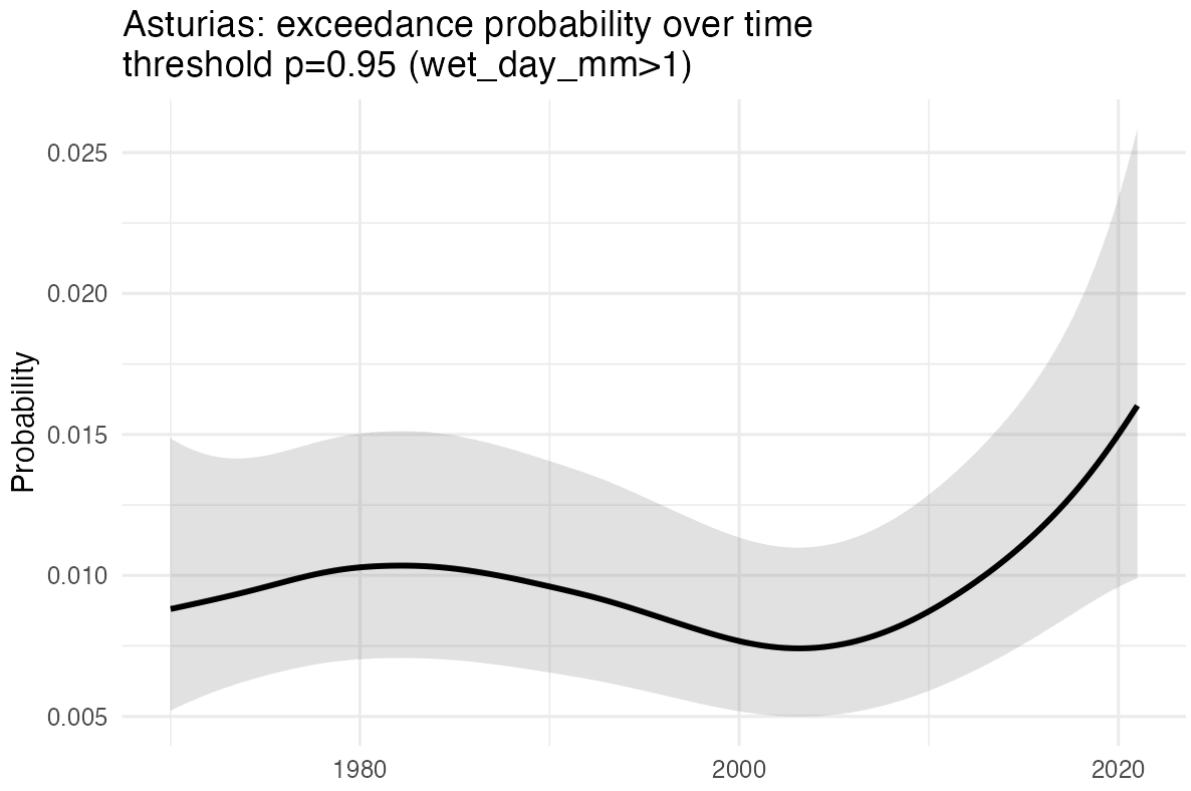
Asturias: exceedance probability over time
threshold p=0.95 (wet_day_mm>1)
Probability
0.025
0.020
0.015
0.010
0.005
1980
2000
2020

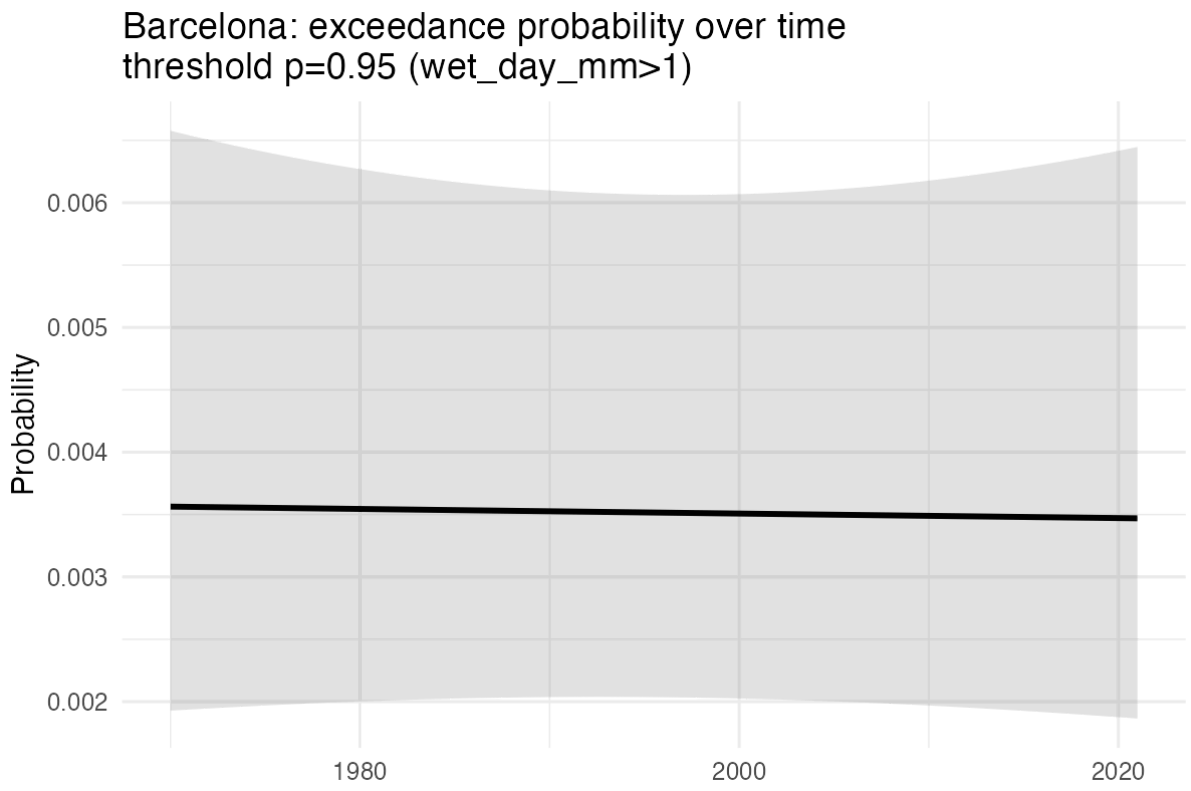
Barcelona: exceedance probability over time
threshold p=0.95 (wet_day_mm>1)
Probability
0.006
0.005
0.004
0.003
0.002
1980
2000
2020

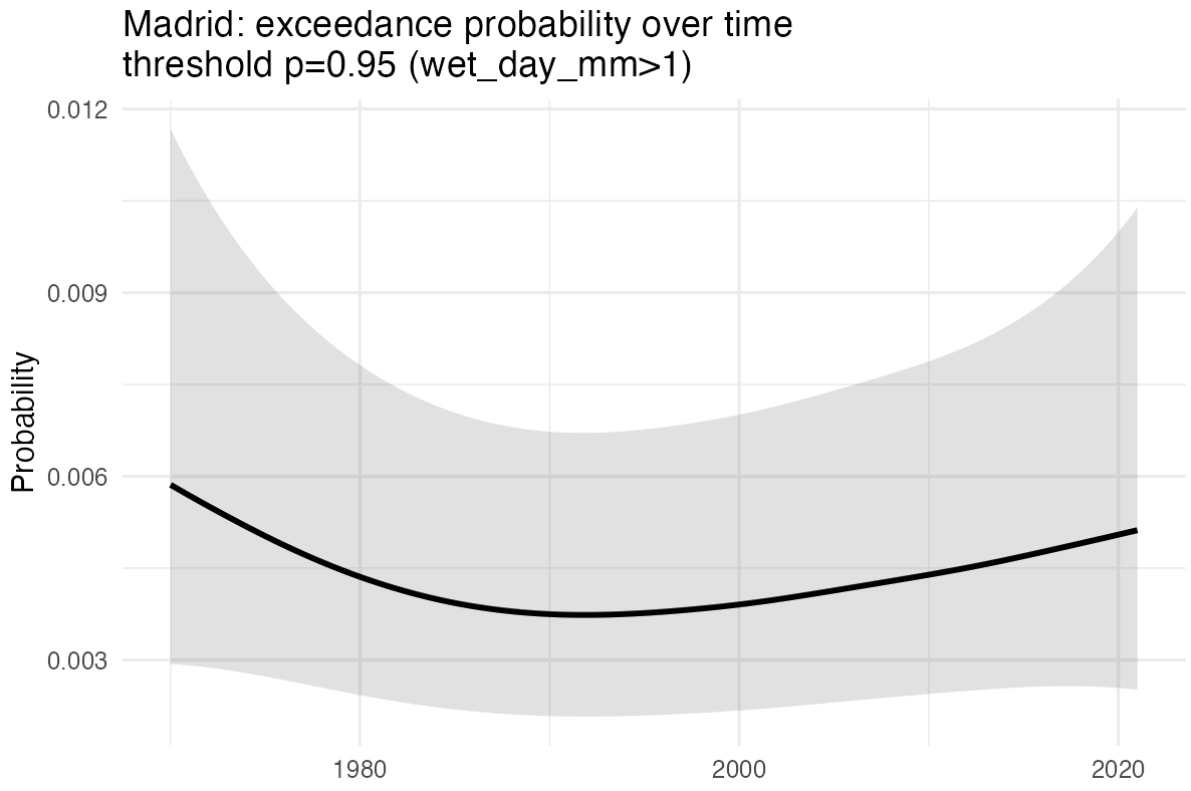
Madrid: exceedance probability over time
threshold p=0.95 (wet_day_mm>1)
Probability
0.012
0.009
0.006
0.003
1980
2000
2020

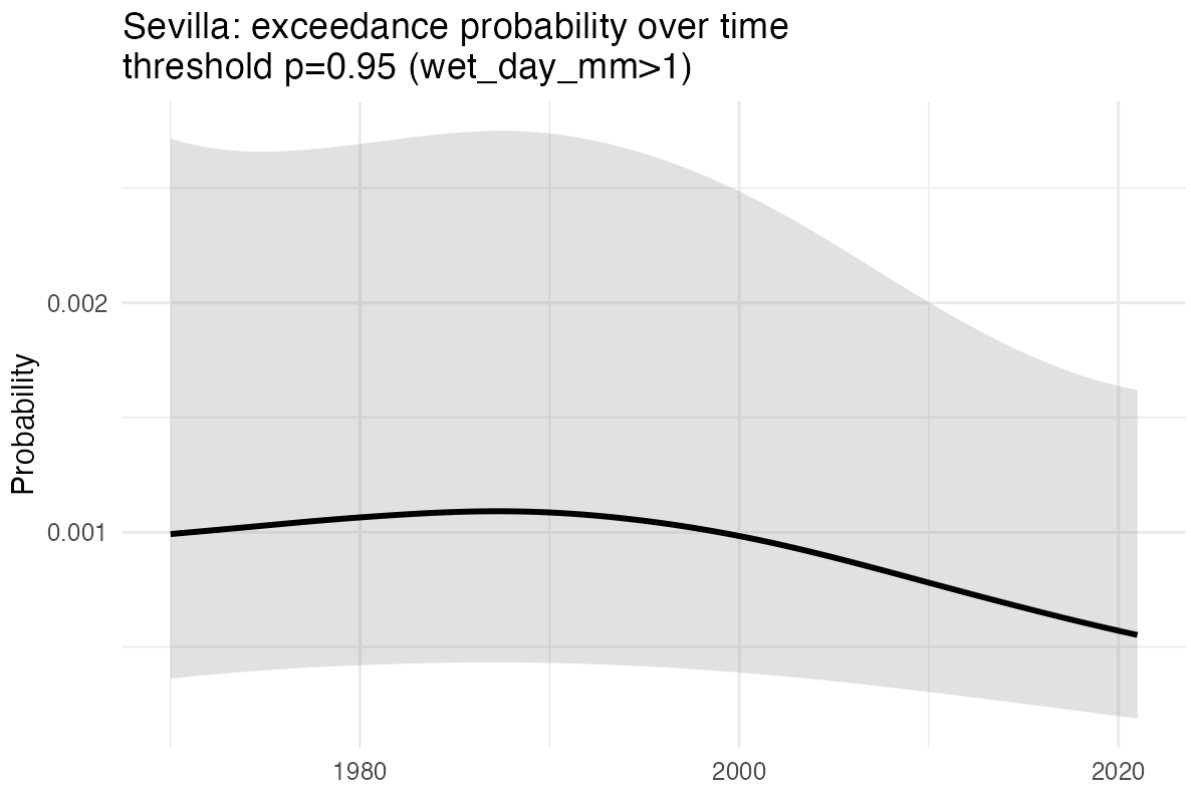
Sevilla: exceedance probability over time
threshold p=0.95 (wet_day_mm>1)
Probability
0.002
0.001
1980
2000
2020

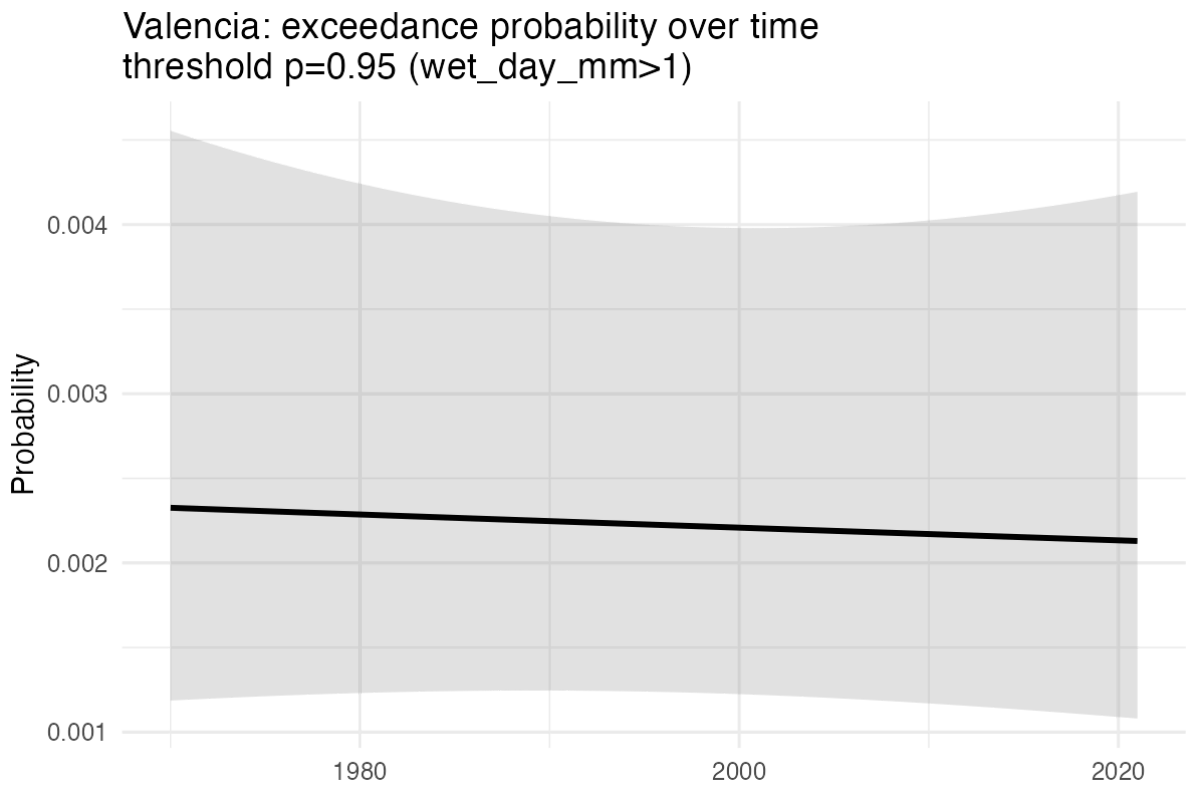

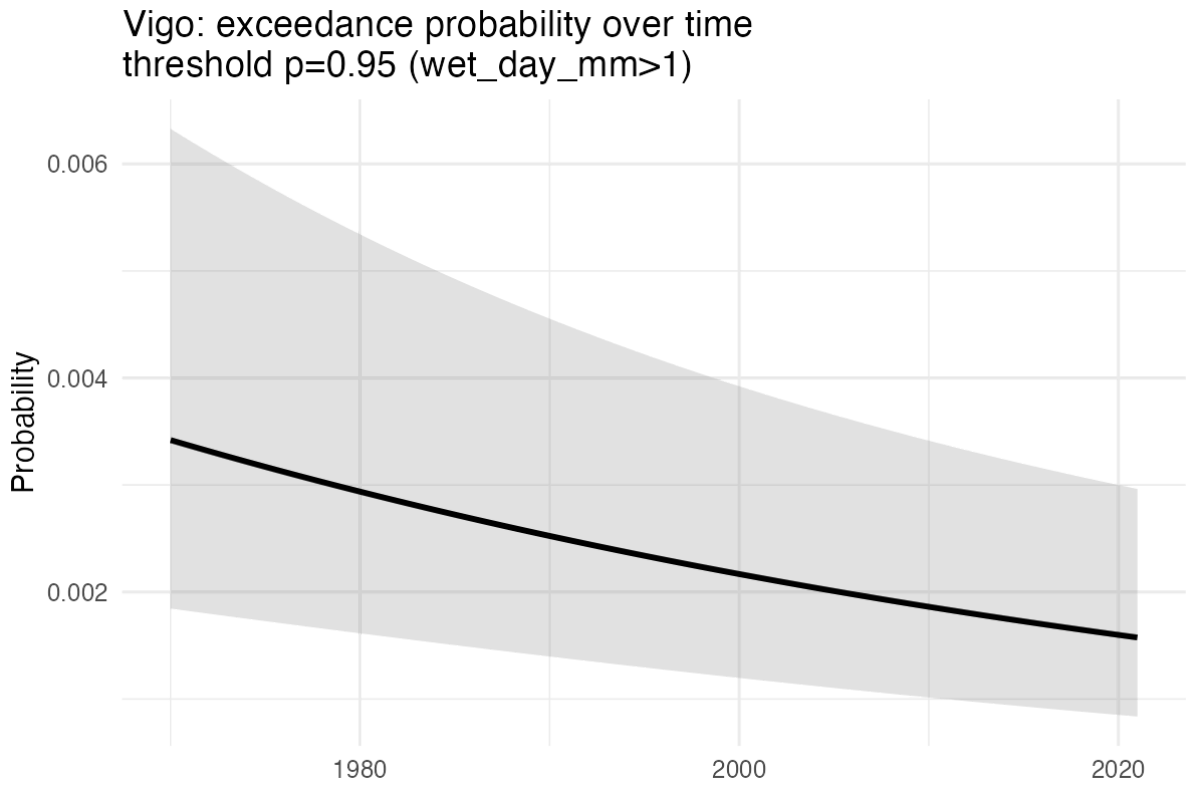

Appendix 4: Output of the Menn-Kandell test on 6 weather stations on the precipitation trend

station	n_years	mk_tau	mk_p	sen_slope_mm_per_year
<chr>	<int>	<dbl>	<dbl>	<dbl>
1 Vigo	51	-0.273	0.00482	-9.47

```
2 Sevilla         51 -0.115  0.236                -2.15
3 Asturias        51 -0.106  0.276                -1.96
4 Barcelona       51 -0.0698 0.475                -0.791
5 Madrid          51 -0.0259 0.795                -0.231
6 Valencia        51  0.0102 0.922                 0.116
```

Appendix 5: climate zones in Spain

Appendix 6: Diversification diagnostics

pair	joint_rate	joint_events
asturias–vigo	0.0574669187145558	152
madrid–vigo	0.0279773156899811	74
sevilla–vigo	0.0279773156899811	74
madrid–sevilla	0.0260869565217391	69
barcelona–asturias	0.0238185255198488	63
asturias–sevilla	0.023062381852552	61
madrid–asturias	0.0219281663516068	58
barcelona–valencia	0.0219281663516068	58
alicante–valencia	0.0196597353497164	52
madrid–barcelona	0.0173913043478261	46
barcelona–vigo	0.0162570888468809	43
madrid–valencia	0.0155009451795841	41
barcelona–alicante	0.0132325141776938	35
barcelona–sevilla	0.012476370510397	33
asturias–valencia	0.0120982986767486	32
sevilla–valencia	0.0109640831758034	29
asturias–alicante	0.00982986767485822	26
madrid–alicante	0.00907372400756144	24

vigo–valencia	0.00680529300567108	18
sevilla–alicante	0.00604914933837429	16
vigo–alicante	0.00491493383742911	13

Appendix 5:

Joint exceedance k >= 3 folds

Front page

Include the title, authors, case designer, abstract and optionally a table of contents.

Abstract (150 - 200 words): provide a concise summary of the research question, method-

ology, key findings, and conclusions; this part should be specific to the case and not include

any literature or examples.

1. Introduction (± 1 – 1.5 pages)

Provide motivation for the research question/goal and its relevance (which should be more

extensive and more general than the abstract).

Include background information on the company, institute, or research department.

Describe the data, chosen methods and models, and give a brief overview of main findings

and implications.

Literature: mention some key references related to the case, and highlight how the report

contributes to it.

End with a short reading guide ("The remainder of this report is organized as follows ...").

2. Data (± 2 – 3 pages)

Describe the data source, data characteristics, and any necessary data preparation.

Include graphs and tables (descriptive statistics) in the main text, with self-explanatory

captions, and a detailed discussion of these findings.

Present it in your own words and with proper mathematical notation. Screenshots or

direct copies of software output are not permitted.

3. Methodology (± 2 – 3 pages)

Specify ´and explain the methods and models used (carefully introducing mathematical

notation), citing relevant literature, and provide a small example where possible.

Present it in your own words, screenshots are not permitted.

Discuss the key assumptions and their validity.

2

Focus on the motivation behind your chosen methods rather than technical derivations.

Preferably also justify why some competitive methods or models were not chosen.

4. Results (± 4 – 5 pages)

Present and discuss the main findings in detail.

Include graphs and tables in the main text, with self-explanatory captions, and extensively describe these results, including a detailed interpretation and careful discussion of implications.

Present it in your own words and with proper mathematical notation. Screenshots or direct copies of software output are not permitted.

If applicable: assumption testing and residual analysis.

5. Conclusion (± 1 – 1.5 pages)

Recap research question/goal, data, methodology, and key findings.

Explain the contribution: what is the relevancy and how does it compare to the literature.

Discuss any limitations of existing research and provide suggestions for future research.

References

Include sufficient references to academic literature (at least three citations in the intro-

duction and at least two in the methodology section).

Use APA-style or ASA-style for citations.

Avoid using footnotes for referencing literature.

A. Appendix

If applicable: for technical explanations, additional results and robustness checks.

Also see the second check box of the Lay-out section (ensure that all necessary content is

included in the main body of the report, as the grade will largely depend on the first 12

pages).

As a first benchmark, a linear probability model (LPM) is estimated using ordinary least squares. The LPM specifies the exceedance probability as a linear function of time, $p_{s,t} = \alpha_s + \beta t + \varepsilon_{s,t}$, where t captures long-run changes in exceedance risk. The LPM is attractive as a baseline since it is easy to model and interpret: the coefficient β directly represents the change in exceedance probability associated with a one-unit increase in time.

However, the LPM has important limitations in this setting. First, fitted values are not constrained to the [0,1] interval, and may thus produce invalid probability predictions. Secondly, the models linear nature fails

Our LPM uses ordinary least squares (OLS) to model the threshold exceedance over time and is able to define a global trend in the probability. However an LPM can compute probabilities outside of the [0,1] range which produces invalid results. Next to that OLS will find a constant coefficient over time and will therefore get bad results in the residual analysis (Mukherjee, 2025).

3.2 Logit & Probit

Logit and Probit are known for their ability to make probabilities bounded and therefore improve the quality of results. As McCullagh en Nelder (p.13, 1989) state in their book about Probit: "This model has the virtue that it respects the property that π_x is a probability and hence must lie between 0 and 1 for all values of x and for all parameter values. The standard formulas for Logit and Probit are as follows (Schmelzer, 2025):

$$probit: \pi_x = \phi(\alpha + \beta x)$$

$$logit: \pi_x = \frac{e^{(\alpha+\beta x)}}{1+e^{(\alpha+\beta x)}}$$

Where π is the probability of x, Φ is the cumulative standard normal distribution function and α and β are the regressors.

3.3 Generalized Additive Model (GAM)

While Generalized Linear Models (GLMs) such as the Logit,probit model improve the LMP problem by adding constraining predictions to the [0,1] interval. The models are still strictly looking for a linear relationship between predictions and the link function of the outcome. Therefore the model will try and force a straight line through the data. ()

The Generalized Additive Model (GAM) extends the GLM framework by replacing the linear predictor with a sum of smoothing functions. The structure is defined as:

The GAM is based on a simple method as explained in *GAM: The Predictive Modeling Silver Bullet* by Kim Larsen:

- Relationships between the individual predictors and the dependent variable follow smooth patterns that can be linear or nonlinear.
- We can estimate these smoothing relationships simultaneously and then predict g(E(y)) by simply adding them up. (Kim Larsen,)

The smoothing functions are

OVERIG

4.1 General trends in precipitation

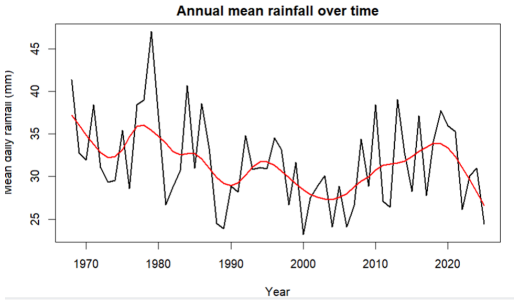

Figure? Trend in Asturias

From the research of Spanjers et al. (2025) we would expect dry weather in southern Europe as a conclusion of a positive NAO-phase. The upwards trend in persistence of positive NAO-phases would therefore lead to a negative trend in precipitation in Spain. This is shown in the graph above containing data of precipitation in Asturias. Asturias lies in North-west Spain and has an oceanic climate with much rain on average following from the map in appendix 5.

Although the negative trend is also found in Sevilla and Barcelona, this does not count for the entirety of Spain. In Alicante for example there is no clear significant trend in the data. Alicante is located on the other side of Spain and has a mediterranean climate. The same result counts for Valencia and Madrid with other climates. Further research is needed to find trends in the data on specific climates in Spain.

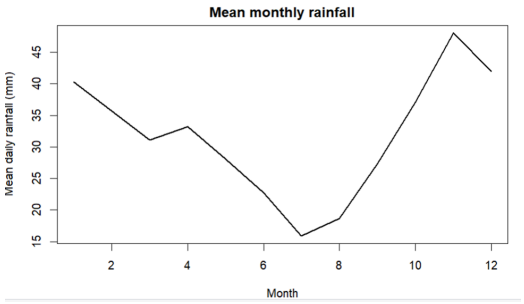

Figure? Seasonality in Asturias

One clear conclusion from the data is the seasonality. **Appendix**? shows the seasonal pattern of rainfall in Asturias. The precipitation in the summer months is near zero and in autumn it is at its peak. The same is visible in the other weather stations throughout Spain.

We also looked at the trend in precipitation over the years with the Mann-Kendall trend test. The test output showed a significant decrease in precipitation on a 99% significance level in Vigo, but the other weather stations all had a clear insignificant trend as shown in Appendix 4.

Oude stuk over GAM

3.3.1 Model specification

In this case there must be d

To model time-varying exceedance probabilities while allowing for non-linear seasonal and long-term patterns, this study uses a generalized additive model, GAM. GAMs are an extension of Generalized Linear Models (GLMs), in which some of the terms in the model are replaced by non-linear functions. The underlying data affects the shape of the smooth function (Underwood, 2009). This suits precipitation data, where long-term trends and seasonal effects are rarely linear and may evolve over time.

The first step for modelling the GAM is to denote $RR_{s,t}$ as the daily precipitation at station *s* on day *t*. A wet day is defined as $RR_{s,t} > 1mm$. For each station, extreme precipitation is identified using wet-day conditioned percentile threshold u_s (baseline p=0.95). The daily exceedance binary variable is then defined as $Y_{s,t} = 1\{RR_{s,t} > u_s\}$, which takes the value of one if an extreme precipitation event occurs and zero otherwise. Conditional on covariates, $Y_{s,t}$ follows a Bernoulli distribution with success probability $p_{s,t}$. The GAM is specified with a logit link function such that $logit(p_{s,t}) = \eta_{s,t}$. This forces bounded probabilities for our outcome.

The non-linear relationships are modelled using penalized regression splines. In this research two different types of spines are used, **Thin Plate Regression Splines** and the **Cyclic Cubic regression splines.** The thin plate regression splines are used for the time trend. These provide an approximation of smooth relationships without the need for manual knot selection.The Cyclic Cubic regression splines are used for the seasonal component, the day of the year. The splines construct a flexible, smooth curve by joining together multiple simpler polynomial segments at specific points, allowing the model to fit non-linear data patterns (Underwood, 2009).

The splines are controlled by a smoothing parameter, which decides how "stiff" the fitted functions are. If this parameter is too low, the model tends to overfit the data by tracking daily noise; if the parameter is too high, the resulting curve becomes too rigid, leading to underfitting. Therefore, finding an optimal balance is crucial. In this study, the smoothing parameters are estimated using Restricted Maximum Likelihood (REML). While choosing the parameter with the lowest Akaike Information Criterion (AIC) is another common method for parameter selection, REML is preferred for this analysis. REML treats the smoothing penalty as a variance component, making it more robust against overfitting particularly when

modelling binary data, where AIC is known to occasionally produce spuriously wiggly functions (Wood, 2011).

Climate change has been associated with an increase in extreme weather events across Europe, including more intense precipitation (Donat et al., 2016; IPCC 2021). For example, Allen & Ingram (2002) have shown that rising temperatures increase the moisture-holding capacity of the atmosphere, thereby raising the potential intensity of precipitation events.

In addition, changes in large-scale atmospheric circulation patterns, most notably the North Atlantic Oscillation, contribute to shifts in regional precipitation behaviour. The NAO measures the pressure difference between the Azores high and the Icelandic low. A positive NAO-phase is generally associated with increased precipitation in north-western Europe, and colder and drier conditions in southern Europe. A negative NAO-phase will result in the opposite pattern (Trigo et al., 2002). An increase in the absolute value of the NAO-index could lead to more phases with heavier precipitation (Spanjers et al., 2025).

These trends exacerbate the operational risk many industries already face because of precipitation. Industries such as agriculture, tourism or construction often benefit from covering downside risks related to precipitation. They increasingly make use of parametric rain insurance, which pays the client if rain levels exceed a predetermined threshold.

Therefore, insurers must have models that are able to correctly estimate the probability of rain exceeding certain thresholds at any given day in the year for differing locations throughout Europe in order not to underwrite at a loss. Additionally, insurers must be sure they have a sufficiently diversified geographical portfolio. Any portfolio is inherently correlated: rainfall exceeding a threshold in the Netherlands increases the probability that rainfall also exceeds that threshold in Germany (Bracken et al., 2016). However, an operational risk for insurers may be that the correlation between geographies is much higher in tail events where precipitation is heavy. This would introduce serious risk of a mass-payout event which can financially strain underwriters.

Therefore, the research aims to answer three main questions:

1. *What is the probability that precipitation crosses the 95th wet day percentile at any given day in the year for Spanish weather stations, and is there evidence of this probability changing over time?*
2. *Is there evidence of the daily probability of spatially correlated joint precipitation exceedances above the 95th percentile across Spain changing over time?*

3. *Which weather station pairs exhibit weakest/strongest diversification, and how does this relate to climate regimes?*

While prior studies document increasing precipitation extremes (Donat et al., 2016) and the role of large-scale circulation patterns such as the NAO (Trigo et al., 2002; Spanjers et al., 2025), this report builds on that literature by translating these climatological insights into a threshold-exceedance analysis directly relevant for parametric insurance providers. This report contributes by modelling time-varying exceedance probabilities and spatially correlated joint exceedances using station-level precipitation data from Spain.

This report will contain sections for the data and methodology. Afterwards, the results will be presented including graphs and tables for better understanding. The report will end with a brief conclusion of the findings and a final answer to the research questions.